ELSEVIER

Toxicology 173 (2002) 193–201

TOXICOLOGY

www.elsevier.com/locate/toxicol

Protein adducts of malondialdehyde and 4-hydroxynonenal in livers of iron loaded rats: quantitation and localization

M. Firoze Khan *, Xiaohong Wu, Ulka R. Tipnis, G.A.S. Ansari, Paul J. Boor

Department of Pathology, University of Texas Medical Branch, Galveston, TX 77555-0609, USA

Received 14 September 2001; accepted 7 October 2001

Abstract

Pathophysiological mechanisms for hepatocellular injury, fibrosis and/or cirrhosis in hepatic iron overload are poorly understood. An increase in intracellular transit pool of iron can catalyze peroxidation of lipids to produce reactive aldehydes such as malondialdehyde (MDA) and 4-hydroxynonenal (HNE). Covalent binding of such lipid aldehydes with proteins may cause impairment in cellular function and integrity. This investigation was focused on quantitative determination of MDA and HNE-protein adducts, and to establish a correlation between iron deposition and formation and localization of MDA and HNE-protein adducts, using immunohistochemistry. To achieve iron overload, male SD rats were fed a 2.5% carbonyl iron-supplemented diet for six weeks, while control animals received standard diet. Total iron as well as low molecular weight chelatable iron (LMWC-Fe) in the hepatic tissue of rats fed the iron supplemented diet increased significantly ($\sim$14- and $\sim$15-fold, respectively). Quantitative ELISA for MDA-and HNE-protein adducts showed remarkable increases of 186 and 149%, respectively, in the liver homogenates of rats fed the iron-supplemented diet. Sections of liver stained for iron showed striking iron deposits in periportal (zone 1) hepatocytes, which was less dramatic in midzonal (zone 2) cells. Livers from iron-loaded rats showed strong, diffuse staining for both MDA and HNE adducts, which was highly pronounced in centrilobular (zone 3) hepatocytes, but was also evident in midzonal cells (zone 2). The demonstration of greater formation of both MDA and HNE-protein adducts provides evidence of iron-catalyzed lipid peroxidation in vivo. Although in this model of iron overload there was no evidence of tissue injury, our results provide an account of some of the initiating factors or early molecular events in hepatocellular damage that may lead to the pathological manifestations seen in chronic iron overload.

Keywords: Iron overload; Liver; Lipid peroxidation; Malondialdehyde; 4-Hydroxynonenal; Protein adducts; Immunohistochemistry

1. Introduction

The liver is one of the major sites of iron deposition in iron overload conditions, and massive deposition of iron within hepatocytes can result in hepatocellular injury leading to hepatic

* Corresponding author. Tel.: +1-409-772-6881; fax: +1-409-747-1763.

E-mail address: mfkhan@utmb.edu (M.F. Khan).

0300-483X/02/$ - see front matter
PII: S0300-483X(02)00043-4

fibrosis and/or cirrhosis (Galleano and Puntarulo, 1992; Britton et al., 1994; Pigeon et al., 1999). However, the pathophysiological mechanisms for the hepatocellular injury leading to the development of fibrosis and/or cirrhosis in hepatic iron overload are not well understood although a direct correlation between hepatic iron and hepatic fibrosis has been demonstrated (Isaacson et al., 1961; Risdon et al., 1975). Iron is normally stored in specific proteins (transferrin, ferritin, lactoferrin and haem proteins). However, under various pathological conditions associated with iron overload, it has been postulated that there is an increase in intracellular transit pool of iron (Thomas et al., 1985; Britton et al., 1990). In fact, within the cells a cytosolic pool of low molecular weight chelatable iron (LMWC-Fe) or so-called free iron exists which appears to be catalytically active in initiating free radical reactions (Halliwell and Gutteridge, 1986; Ceccarelli et al., 1995). Iron accumulation in the liver has been shown to be causally related to increased lipid peroxidation (Hultcrantz et al., 1984; Whittaker et al., 1996), which has been proposed as an initial step by which excess iron causes cellular injury (Powell et al., 1980; Bonkovsky et al., 1981). Iron-catalyzed peroxidation of lipids produces reactive aldehydes such as malondialdehyde (MDA) and 4-hydroxynonenal (HNE). Covalent binding of such lipid aldehydes with proteins and the resulting adducts may cause impairment of cellular function and integrity and could be a potential mechanism in iron-induced liver damage, and is the focus of this study. Using rats as an in vivo model of iron overload, this study presents: (a) quantitative assessment of MDA and HNE-protein adducts using enzyme-linked immunosorbent assay (ELISA), and (b) localization patterns of MDA and HNE-protein adducts in liver using immunohistochemistry.

2. Materials and methods

2.1. Animals and diets

Male Sprague–Dawley rats (~ 200 g), obtained from Harlan Sprague–Dawley (Indianapolis, IN), were housed in wire-bottom cages over absorbent paper with free access to tap water and Purina rat chow. The animals were acclimatized in the controlled-environment animal room (temperature, 22 °C; relative humidity, 50%; photoperiod, 12-h light:12-h dark cycle) for 7 days.

The animals were divided into two groups of five rats each and were either fed normal diet or a 2.5% carbonyl iron-supplemented diet (Dyets, Inc, Bethlehem, PA) for 6 weeks [the iron dose and treatment regimen was based on studies of Ceccarelli et al. (1995) who reported most dramatic increases in free iron content at about 6 weeks]. The rats were euthanized under ether anesthesia. All major organs were removed immediately, blotted, weighed and stored at −80 °C until further analysis.

2.2. Total iron and low molecular weight chelatable iron in the liver

Total iron in the livers was analyzed by atomic absorption spectrophotometry as described by Alcock (1987). Analysis of low molecular weight chelatable iron (LMWCFe, free iron) was done as described by Reif et al. (1988) with slight modifications (Khan et al., 1999a). Briefly, liver homogenates (2.5%) were prepared in distilled water containing 1 mM ethylenediamine tetra acetic acid (EDTA). EDTA was added to facilitate the separation of the LMWC-Fe pool. The homogenates were then centrifuged at 20 000 × *g* for 15 min at 4 °C, and the supernatants were filtered on Micron-30 (molecular weight cut off 30 000; Amicon, Inc) at 14 000 × *g* for 20 min at 4 °C. Aliquots were analyzed for iron by Zeeman graphite furnace analysis using an iron hollow-cathode lamp. Protein in the filtrate was determined according to Lowry et al. (1951).

2.3. Preparation of MDA-and HNE-protein adducts and production of polyclonal antibodies

MDA adducts of ovalbumin was prepared essentially as described earlier (Lung et al., 1990; Khan et al., 1997), whereas HNE adducts of ovalbumin was prepared according to Uchida et al. (1993) by reacting 5 mg/ml of ovalbumin with

8.7 mM HNE (Cayman Chemical Co, Ann Arbor, MI) at 37 °C for 4 h. Free amino groups that did not react with MDA or HNE were determined by 2,4,6-trinitrobenzene-1-sulfonic acid assay (Habeeb, 1966). Our results showed that treatment of 5 mg/ml of ovalbumin with 50 mM MDA or 8.7 mM HNE modified about 86 and 60% amino groups, respectively. These preparations were used for generation of polyclonal antibodies. Polyclonal antibodies to MDA-and HNE-ovalbumin were raised in white New Zealand rabbits [Alpha Diagnostics International, San Antonio, TX (Khan et al., 1997)]. These antibodies were highly specific for their respective protein adducts, and did not crossreact with protein adducts of formaldehyde, acetaldehyde, glutaraldehyde or acrolein as assessed by ELISA.

2.4. Quantitation of MDA-and HNE-protein adducts

A quantitative competitive ELISA for MDA-or HNE-protein adducts in the liver homogenates (20%, w/v) of control and iron-treated rats was established. Briefly, flat bottomed 96-well microtiter plates were coated with MDA- or HNE-ovalbumin adducts or ovalbumin (0.5 μg per well) overnight at 4 °C. Rabbit antisera (1:1500 diluted anti-MDA or 1:3000 diluted anti-HNE) were incubated with test samples (standards or unknown) at 4 °C overnight, and then a 50 μl aliquot of each incubation mixture was added to duplicate wells of the coated plates and incubated for 2 h at 37 °C. After washing, 50 μl of goat anti-rabbit IgG-HRP (1:5000 dilution) was added and incubated for 1 h at 37 °C. After washing, 100 μl substrate (tetramethylbenzidine/H2O2)was added to each well. The reaction was stopped after 10 min by adding 100 μl 0.5 M H2SO4 and the absorbance was measured at 450 nm on a microplate reader.

2.5. Immunohistochemical staining for MDA-and HNE-protein adducts

For immunohistochemical localization of MDA and HNE adducts, MDA-and HNE-KLH conjugates were prepared as described above, and polyclonal antibodies to these conjugates were raised in rabbits (Alpha Diagnostics International). Antibodies against KLH conjugates of MDA and HNE had higher titers and greater specificity for the respective aldehydes.

Immunohistochemical staining procedure was extensively standardized for these adducts for their localization in iron-treated livers. Briefly, 4 μm tissue sections were deparafinized in an oven at 55 °C for 1 h and passed through xylene and various concentrations of ethanol, and finally rehydrated with water. The slides were incubated with unmasking buffer (Vector, Burlingame, CA) at 95 °C for 20 min for antigen retrieval and then subsequently incubated with different reagents for blocking the nonspecific binding sites, which included peroxidase inhibitor (Pierce, Rockford, IL) for 15 min, levamisole (alkaline phosphatase inhibitor; 0.2%) for 10 min, 0.5% periodic acid for 5 min, avidin and biotin block solutions (Vector) for 10 min each, and normal serum (Signet, Dedham, MA) for 5 min. The sections were then incubated with rabbit anti-MDA serum or rabbit anti-HNE serum [1:500 dilution in antibody diluent buffer (Dako, Carpinteria, CA)] for 1 h and then anti-rabbit IgG-biotin [1:1200 (Sigma Chemical Co, St. Louise, MO)] for 20 min at room temperature. The slides were thoroughly washed after each incubation. The Signet ultra streptavidin alkaline phosphatase labeling reagent was then added to the tissue sections and incubated for 20 min at room temperature. Finally, Fast Red (Biopathology, Inc, Okalahoma City, OK) staining was performed according to the company's manual. To check the specificity of the staining, set of additional sections were also stained with preimmune serum (1:500 dilution) or antiserum pre-absorbed with MDA- or HNE-ovalbumin. All sections were finally counterstained with hematoxylin (Gill's formulation, Vector) and mounted for examination under light microscopy.

2.6. Histology

A portion of liver from control and treated rats was fixed in 10% neutral-buffered formalin for histological processing. Paraffin sections were cut and stained with hematoxylin and eosin (H&E),

Perl's Prussian blue (iron stain) and Masson's trichrome (for collagen) for morphological evaluation (Khan et al., 1997, 1999b).

2.7. Statistical analysis

All data are expressed as mean ± S.D. Significance of differences was assessed by the Student's *t*-test. A P value of < 0.05 was considered to be statistically significant.

3. Results

3.1. Total iron and LMWC-Fe in the livers

Total iron content in the livers of iron-loaded rats increased substantially, which was ~14-fold (1275%) higher than the controls (Fig. 1). Similarly, LMWC-Fe also increased dramatically with an increase of ~15-fold (1396%) over the controls (Fig. 2).

3.2. MDA-and HNE-protein adducts

Polyclonal antibodies against MDA and HNE adducts, used to establish ELISA for the quantitative assessment of these adducts, were specific for these adducts and did not cross react with protein adducts of acrolein, acetaldehyde or formaldehyde. MDA protein adducts, as quantitated by ELISA, in the liver homogenates of iron loaded rats showed a highly significant increase of 186% in comparison with the controls (Fig. 3). Similarly, the formation of HNE-protein adducts was also significantly greater (149%) in the livers of iron loaded rats (Fig. 4).

3.3. Liver morphology

Liver histology was examined after 6 weeks of iron overload. The sections of liver stained with

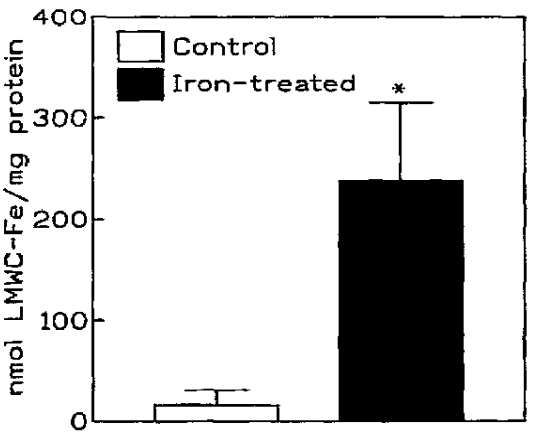

Fig. 2. LMWC-Fe (free iron) in livers of control and iron-treated rats. Values are mean ± S.D. of five animals. *$P < 0.05$ as compared with the controls.

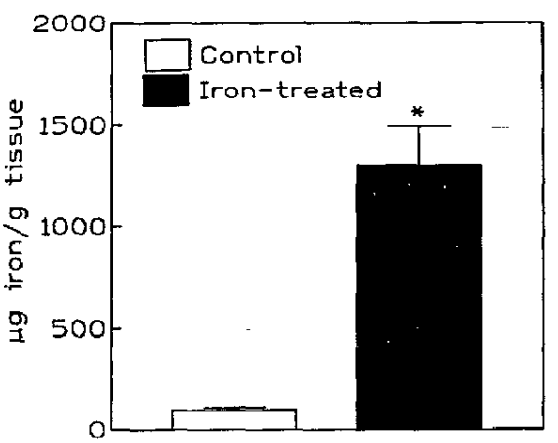

Fig. 1. Total iron content in the livers of control and iron-treated rats. Values are mean ± S.D. of five animals. *$P < 0.05$ as compared with the controls.

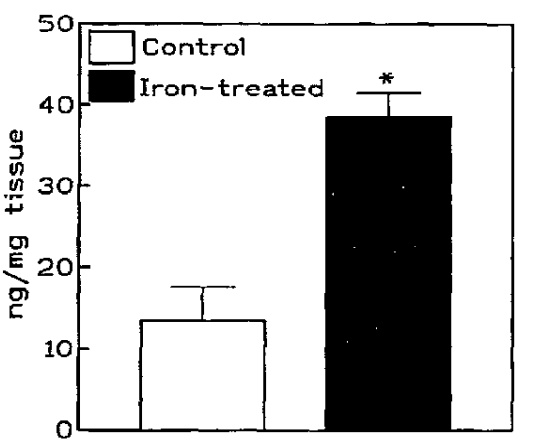

Fig. 3. MDA-protein adducts in the livers of control and iron-treated rats. Values are mean ± S.D. of five animals. *$P < 0.05$ as compared with the controls.

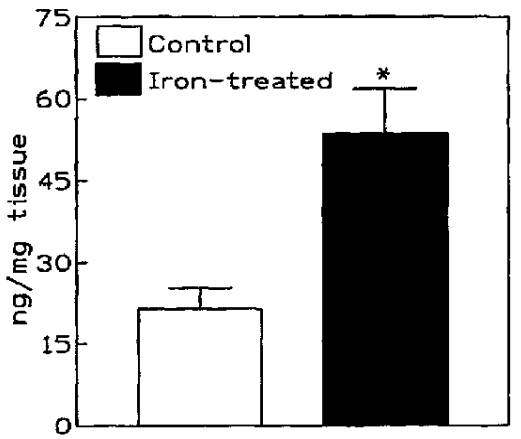

Fig. 4. HNE-protein adducts in livers of control and iron-treated rats. Values are mean ± S.D. of five animals. $^*P < 0.05$ as compared with the controls.

hematoxylin and eosin did not show any evidence of cell injury or a change in the liver architecture. Evaluation of sections stained with Masson's trichrome showed no increase in extracellular matrix production or fibrosis. Evaluation of sections stained with Perl's Prussian blue showed striking iron deposits in hepatocytes, sinusoids and occasionally in Kupffer cells in the livers of iron-loaded rats. Periportal hepatocytes (Zone 1), however, showed maximum deposition of iron in iron-loaded rats (Fig. 5). Control rats showed scanty, minimal iron deposition in random hepatocytes.

3.4. Immunohistochemical localization of MDA-and HNE-protein adducts

Sections of liver were immunohistochemically stained for MDA- and HNE-adducts using polyclonal MDA- and HNE-specific antibodies (see Section 2). Alkaline phosphatase-Fast Red (red color) demonstration of bound primary antibodies provided a sharper and increased contrast compared with horseradish peroxidase-diaminobenzidine (HRP-DAB; brown color) methodology. This method allowed for differentiating the changes in the iron-treated rats, which had extensive brownish deposits of iron, and thus represented a more effective method of localizing protein adducts in iron-loaded tissues. Control livers showed a moderate red staining (Fig. 6B), primarily localized within a few cells immediately adjacent to central vein. Livers from iron-loaded rats showed much stronger, diffuse staining for both MDA and HNE-adducts (Fig. 6A; only HNE staining shown), which was highly pronounced in centrilobular hepatocytes (zone 3). Staining for these adducts was less dramatic in the midzonal hepatocytes and sparse in the periportal hepatocytes. No staining was evident in liver sections incubated with pre-immune serum or antiserum pre-absorbed with MDA- or HNE-ovalbumin.

4. Discussion

Excess iron deposited chronically is associated with hepatic injury, fibrosis and ultimately cirrhosis (Powell et al., 1980; Britton et al., 1994). Despite clinical evidence for the toxicity of excess iron, the specific cytopathological mechanisms of hepatocellular injury due to iron overload have not been fully explored and remain inconclusive (Galleano and Puntarulo, 1992). These studies were focused on establishing a quantitative assessment of the formation of adducts of lipid peroxidation products such as MDA and HNE, and a correlation between iron deposition and formation and localization of MDA and HNE-protein adducts. Iron overload in our studies was achieved by supplementing the diet with 2.5% carbonyl iron. The 6-week regimen for iron treatment was based on studies of Ceccarelli et al. (1995) who reported peak values for both total and LMWC-Fe around 40 days. Our data also showed remarkable increases in total iron and LMWC-Fe, and are in agreement with earlier findings (Ceccarelli et al., 1995).

Accumulation of iron, especially free iron, plays an essential role in the development of fulminent hepatitis, hepatic fibrosis and subsequent carcinogenesis in rats (Kato et al., 1996). Increases in hepatic LMWC-Fe are indeed associated with pro-oxidant action (Ceccarelli et al., 1995), presumably due to greater generation of

hydroxyl radicals. In fact, studies of Linpisarn et al. (1991) show that in vivo lipid peroxidation correlated well with the iron concentration in the liver and spleen of iron-overloaded rats. It is thus not surprising that enhanced lipid peroxidation has been proposed as an initial step by which iron causes cellular injury (Bonkovsky et al., 1981; Houglum et al., 1990; Britton, 1996).

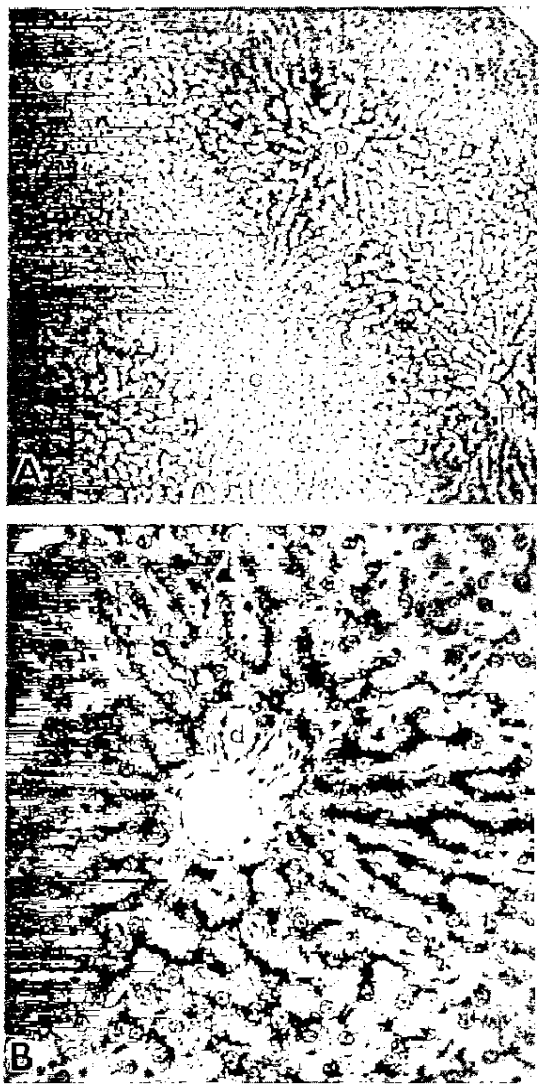

Fig. 5

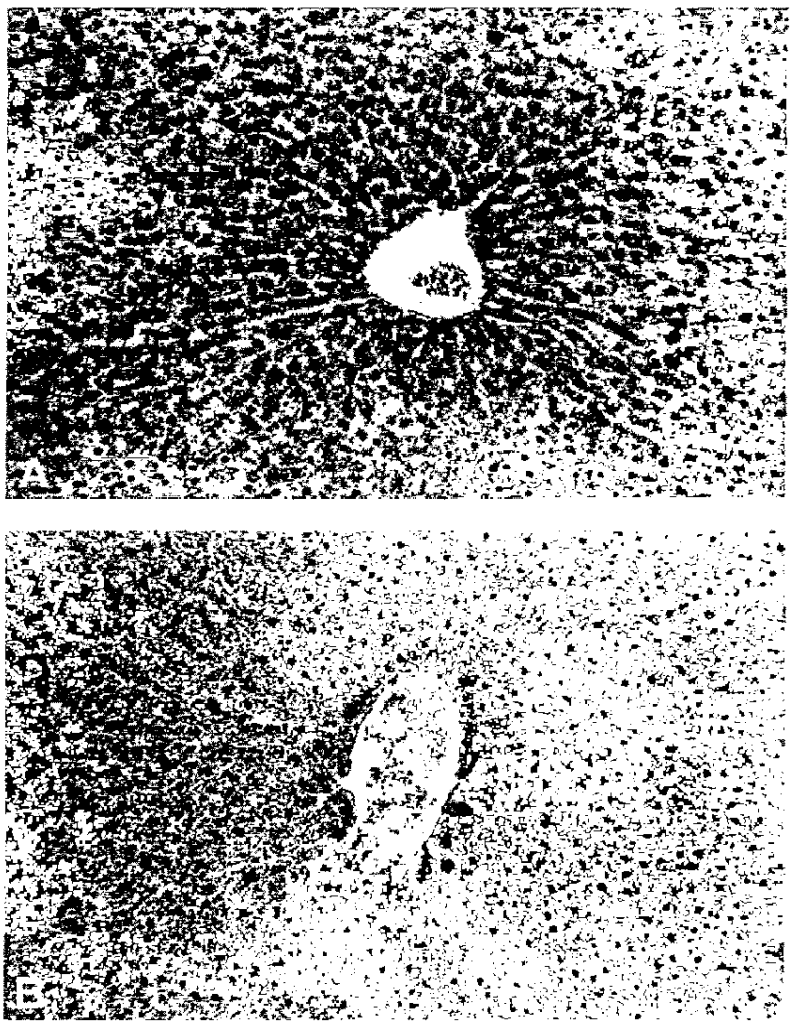

Fig. 6

Fig. 5. Iron deposition in liver. Light micrograph of liver from an iron-treated rat (A) shows marked iron deposition in the hepatocytes of the periportal region (p); central areas (c) show no iron. Higher power view of portal area (B) shows heavy iron deposition within hepatocytes. Note characteristic appearance of bile duct (d) within portal area. Perl's Prussian blue stain; A: × 50; B: × 220.

Fig. 6. Immunohistochemical detection of iron-induced formation of MDA-and HNE-protein adducts in liver. A central vein is present in the center of each photomicrograph (× 200). Livers from iron-treated rats show strong staining for HNE-protein adducts (shown here) as well as similar staining for MDA-protein adducts (not shown). Zone 3 hepatocytes stain most intensely with staining extending to zone 2, whereas zone 1 hepatocytes are unstained. Control liver (B) shows focal, mild staining for HNE-protein adducts localized within a few cells adjacent to central vein.

Chelation of hepatic iron by desferrioxamine has been shown to reduce liver injury caused by lipid peroxidation, leading to reduction of preneoplastic lesions (Sakaida et al., 1999).

The process of lipid peroxidation generates numerous cytotoxic degradation products such as MDA and HNE (Esterbauer et al., 1991), which can form covalent adducts with proteins, phospholipids and DNA (Sodum and Chung, 1988; Houglum et al., 1990; Toyokuni et al., 1995; Guichardant et al., 1998). Our ELISA data showed significant increases both in MDA as well as HNE-protein adducts in the liver as a result of iron overload and reflect increased oxidative modification of tissue proteins in vivo. The increased formation of these adducts also suggests that significant proportion of these toxicants escape detoxification in vivo to form adducts with tissue macromolecules, which may lead to tissue damage.

Iron-specific staining in our studies showed greater presence of iron in hepatocytes of the periportal area (zone 1) and to lesser extent in zone 2. In contrast to iron, however, both MDA and HNE-protein adducts showed greater immunostaining in zone 3, with some staining in cells of zone 2. Variable hepatic localization patterns (zone 1, 2 or 3) for these adducts have been reported as a result of exposure to a number of toxicants (Houglum et al., 1990; Ohhira et al., 1998; Hartley et al., 1999) and it would appear that the nature of the toxicant and the duration of exposure could contribute to their diversified localization. Also liver iron demonstrated by Perls' Prussian blue reaction is protein-bound iron, such as hemosiderin and ferritin (Ohhira et al., 1998). Therefore, this bound iron may be inactive to generate free radicals, and it would appear that release of free, reactive iron is essential for the formation of tissue-damaging free radicals. It is evident from our studies that increases in free iron (LMWC-Fe) is clearly associated with enhanced production of aldehyde adducts as a result of enhanced iron-catalyzed lipid peroxidation. The greater formation of these adducts along with reports of the presence of both MDA and HNE adducts in liver biopsies from patients with genetic hemochromatosis and hepatitis C (Niemela et al., 1995; Paradis et al., 1997) are of vital significance since formation of these adducts may cause impairment in cellular function and integrity and present a potential mechanism in iron-induced hepatic injury. The subcellular localization of these adducts and the identification of modified protein(s) would shed further light on their possible role in tissue injury. For example, adduction of HNE with cytochrome C oxidase in rat liver mitochondria is indeed accompanied by loss of enzyme activity (Chen et al., 1998), and has been proposed as one of the mechanisms of mitochondrial damage caused by oxidative stress. Iron overload in our rat model (only 6-week treatment) did not result in any overt hepatic cell damage or noticeable change in the extracellular matrix production, which is in agreement with Hultcrantz et al. (1984) and could be attributed to the short duration of iron treatment. Chronic studies, however, suggest a significant correlation between iron accumulation and collagen synthesis, stimulated by iron-induced lipid peroxidation (Poli and Parola, 1996).

In conclusion, using this rat model of experimental iron overload, we have demonstrated a positive correlation between free iron and formation of MDA and HNE adducts. The formation of these adducts not only provides an evidence of iron catalyzed lipid peroxidation in vivo, but also provides an account of some of the initiating factors or early molecular events in hepatocellular damage that may lead to the pathological manifestations observed in chronic overload conditions.

Acknowledgements

This publication was made possible by grant number ES 06476 from the National Institute of Environmental Health Sciences (NIEHS), NIH and its contents are solely the responsibility of the authors and do not necessarily represent the official views of the NIEHS, NIH. The authors wish to thank Kerry Graves for his help in establishing the immunostaining method.

References

Alcock, N.W., 1987. A hydrogen peroxide digestive system for tissue trace metal analysis. Biol. Trace Elem. Res. 13, 363–370.

Bonkovsky, H.L., Healey, J.F., Sinclair, P.R., Sinclair, J.F., Pomeroy, J.S., 1981. Iron and the liver. Acute and long-term effects of iron-loading on hepatic haem metabolism. Biochem. J. 196, 57–64.

Britton, R.S., 1996. Metal-induced hepatotoxicity. Semin. Liver Dis. 16, 3–12.

Britton, R.S., Ferrali, M., Magiera, C.J., Recknagel, R.O., Bacon, B.R., 1990. Increased prooxidant action of hepatic cytosolic low-molecular-weight iron in experimental iron overload. Hepatology 11, 1038–1043.

Britton, R.S., Ramm, G.A., Olynyk, J., Singh, R., O'Neill, R., Bacon, B.R., 1994. Pathophysiology of iron toxicity. Adv. Exp. Med. Biol. 356, 239–253.

Ceccarelli, D., Gallesi, D., Giovannimi, F., Ferrali, M., Masini, A., 1995. Relationship between free iron level and rat liver mitochondrial dysfunction in experimental dietary iron overload. Biochem. Biophy. Res. Commun. 209, 53–59.

Chen, J., Schenker, S., Frosto, T.A., Henderson, G.I., 1998. Inhibition of cytochrome C oxidase activity by 4-hydroxynonenal (HNE). Role of HNE adduct formation with the enzyme subunits. Biochim. Biophys. Acta 1380, 336–344.

Esterbauer, H., Schus, R.J., Zollner, H., 1991. Chemistry and biochemistry of 4-hydroxynonenal, malonaldehyde and related aldehydes. Free Radical Biol. Med. 11, 81–128.

Galleano, M., Puntarulo, S., 1992. Hepatic chemiluminescence and lipid peroxidation in mild iron overload. Toxicology 76, 27–38.

Guichardant, M., Taibi-Tronche, P., Fay, L.B., Lagarde, M., 1998. Covalent modifications of aminophospholipids by 4-hydroxynonenal. Free Radic. Biol. Med. 25, 1049–1056.

Habeeb, A.R.S.A., 1966. Determination of free amino groups in proteins by trinitrobenzenesulfonic acid. Anal. Biochem. 14, 328–336.

Halliwell, B., Gutteridge, J.M.C., 1986. Oxygen free radicals and iron in relation to biology and medicine: some problems and concepts. Arch. Biochem. Biophys. 246, 501–514.

Hartley, D.P., Kolaja, K.L., Reichard, J., Petersen, D.R., 1999. 4-Hydroxynonenal and malondialdehyde hepatic protein adducts in rats treated with carbon tetrachloride: immunochemical detection and lobular localization. Toxicol. Appl. Pharmacol. 161, 23–33.

Houglum, K., Filip, M., Witztum, J.L., Chojkier, M., 1990. Malondialdehyde and 4-hydroxynonenal protein adducts in plasma and liver of rats with iron overload. J. Clin. Invest. 86, 1991–1998.

Hultcrantz, R., Ericsson, J.L.E., Hirth, T., 1984. Levels of malondialdehyde production in rat liver following loading and unloading with iron. Virchows Arch. Cell. Pathol. 45, 139–146.

Isaacson, C., Seftel, H.C., Keeley, K.J., Bothwell, T.H., 1961. Siderosis in the Bantu: the relationship between iron overload and cirrhosis. J. Lab. Clin. Med. 58, 845–853.

Kato, J., Kobune, M., Kohgo, Y., Sugawara, N., Hisai, H., Nakamura, T., Sakamaki, S., Sawada, N., Niitsu, Y., 1996. Hepatic iron deprivation prevents spontaneous development of fulminant hepatitis and liver cancer in Long–Evans Cinnamon. J. Clin. Invest. 98, 923–929.

Khan, M.F., Wu, X., Alcock, N.W., Boor, P.J., Ansari, G.A.S., 1999a. Iron exacerbates aniline-associated splenic toxcity. J. Toxicol. Environ. Health 57, 173–184.

Khan, M.F., Wu, X., Boor, P.J., Ansari, G.A.S., 1999b. Oxidative modification of lipids and proteins in aniline-induced splenic toxicity. Toxicol. Sci. 48, 134–140.

Khan, M.F., Wu, X., Kaphalia, B.S., Boor, P.J., Ansari, G.A.S., 1997. Acute hematopoietic toxicity of aniline in rats. Toxicol. Lett. 92, 31–37.

Linpisarn, S., Satoh, K., Mikami, T., Orimo, H., Shinjo, S., Yoshino, Y., 1991. Effects of iron on lipid peroxidation. Int. J. Hematol. 54, 181–188.

Lowry, O.H., Rosebrough, N.J., Farr, A.L., Randall, R.J., 1951. Protein measurement with the folin phenol reagent. J. Biol. Chem. 193, 265–275.

Lung, C.C., Fleisher, J.H., Meinke, G., Pinnas, J.L., 1990. Immunochemical properties of malondialdehyde-protein adducts. J. Immunol. Methods 128, 127–132.

Niemela, O., Parkkila, S., Britton, R.S., Ramm, G.S., O'Neill, R., Janney, C.G., Brunt, E.M., Bacon, B.R., 1995. Hepatic lipid peroxidation in patients with hereditary hemochromatosis. Hepatology 22, 372A.

Ohhira, M., Ohtake, T., Matsumoto, A., Saito, H., Ikuta, K., Fujimoto, Y., Ono, M., Toyokuni, S., Kohgo, Y., 1998. Immunochemical detection of 4-hydroxy-2-nonenal modified-protein adducts in human alcoholic liver diseases. Alcohol Clin. Exp. Res. 22, 145S–149S.

Paradis, V., Mathurin, P., Kollinger, M., Imbert-Bismut, F., Charlotte, F., Piton, A., Opolon, P., Holstege, A., Poynard, T., Bedossa, P., 1997. In situ detection of lipid peroxidation in chronic hepatitis C: correlation with pathological features. J. Clin. Pathol. 50, 401–406.

Pigeon, C., Turlin, B., Iancu, T.C., Leroyer, P., LeLan, J., Deugnier, Y., Brissot, P., Loreal, O., 1999. Carbonyl-iron supplementation induces hepatocyte nuclear changes in BALB/CJ male mice. J. Hepatol. 30, 926–934.

Poli, G., Parola, M., 1996. Oxidative damage and fibrogenesis. Free Radic. Biol. Med. 22, 287–305.

Powell, L.W., Bassett, M.L., Halliday, J.W., 1980. Hemochromatosis: 1980 update. Gastroenterology 78, 374–381.

Reif, D.W., Beales, I.L.P., Thomas, C.E., Aust, S.D., 1988. Effect of diquat on the distribution of iron in rat liver. Toxicol. Appl. Pharmacol. 93, 506–510.

Risdon, R.A., Barry, M., Flynn, D.M., 1975. Transfusional iron overload: the relationship between tissue iron concentration and hepatic fibrosis in thalassemia. J. Pathol. 116, 83–95.

Sakaida, I., Hironaka, K., Uchida, K., Okita, K., 1999. Iron chelator deferoxamine reduces preneoplastic lesions in liver induced by chloine-deficient L-amino acid defined diet in rats. Digest. Dis. Sci. 44, 560–569.

Sodum, R.S., Chung, F.-L., 1988. 1, N2-Etheno-deoxyguanosine as a potential marker for DNA adduct formation by trans-4-hydoxy-2-nonenal. Cancer Res. 48, 320–323.

Thomas, C.E., Morehouse, L.A., Aust, S.D., 1985. Ferritin and superoxide-dependent lipid peroxidation. J. Biol. Chem. 260, 3275–3280.

Toyokuni, S., Miyake, N., Hiai, H., Hagiwara, M., Kawakishi, S., Osawa, T., Uchida, K., 1995. The monoclonal antibody specific for the 4-hydroxy-2-nonenal histidine adduct. FEBS Lett. 359, 189–191.

Uchida, K., Szweda, L.I., Chae, H.-Z., Stadtman, E.R., 1993. Immunochemical detection of 4-hydroxynonenal protein adducts in oxidized hepatocytes. Proc. Natl. Acad. Sci. USA 90, 8742–8746.

Whittaker, P., Hines, F.A., Robl, M.G., Dunkel, V.C., 1996. Histopathological evaluation of liver, pancreas, spleen, and heart from iron-overloaded Sprague–Dawley rats. Toxicol. Pathol. 24, 558–563.